Review of Scientific Instruments

A novel characterization technique for superparamagnetic iron oxide nanoparticles: The superparamagnetic quantifier, compared with magnetic particle spectroscopy

Cite as: Rev. Sci. Instrum. **90**, 024101 (2019); https://doi.org/10.1063/1.5039150
Submitted: 07 May 2018 . Accepted: 12 January 2019 . Published Online: 01 February 2019

M. M. van de Loosdrecht, S. Draack, S. Waanders, J. G. L. Schlief, H. J. G. Krooshoop, T. Viereck, F. Ludwig, and B. ten Haken

AIP Publishing

Review of Scientific Instruments ARTICLE scitation.org/journal/rsi

A novel characterization technique for superparamagnetic iron oxide nanoparticles: The superparamagnetic quantifier, compared with magnetic particle spectroscopy

Cite as: Rev. Sci. Instrum. 90, 024101 (2019); doi: 10.1063/1.5039150
Submitted: 7 May 2018 • Accepted: 12 January 2019 •
Published Online: 1 February 2019

M. M. van de Loosdrecht,[1,a)] S. Draack,[2] S. Waanders,[1] J. G. L. Schlief,[1] H. J. G. Krooshoop,[1] T. Viereck,[2] F. Ludwig,[2] and B. ten Haken[1]

AFFILIATIONS

[1] Magnetic Detection and Imaging group, Faculty of Science and Technology, University of Twente, Enschede, The Netherlands
[2] Institut für Elektrische Messtechnik und Grundlagen der Elektrotechnik, TU Braunschweig, Braunschweig, Germany

[a)] m.m.vandeloosdrecht@utwente.nl

ABSTRACT

Superparamagnetic iron oxide nanoparticles (SPIONs) are used as a tracer material in sentinel node biopsies. The latter is a procedure to analyze if cancer cells have spread to lymph nodes, helping to personalize patient care. To predict SPION behavior *in vivo*, it is important to analyze their magnetic properties in biological environments. The superparamagnetic quantifier (SPaQ) is a new device to measure the dynamic magnetization curve of SPIONs. The magnetization curve was measured for two types of SPIONs: Resovist and SHP-25. We used three techniques: Vibrating Sample Magnetometry (VSM), Magnetic Particle Spectroscopy (MPS), and our new SPaQ. Furthermore, AC susceptibility (ACS) measurements were performed as part of the evaluation of the three techniques. SPaQ and VSM results were found to be similar. Measurement results were nearly identical in both directions, indicating minor hysteresis. However, in MPS measurements, a clear hysteresis loop was observed. Furthermore, the ACS measurements showed a pronounced Brownian maximum, indicating an optimal response for an AC frequency below 10 kHz for both particle systems. Both the SPaQ and MPS were found to be superior to VSM since measurements are faster, can be performed at room temperature, and are particularly sensitive to particle dynamics. The main difference between the SPaQ and MPS lies in the excitation sequence. The SPaQ combines an alternating magnetic field that has a low amplitude with a gradual DC offset, whereas MPS uses only an alternating field that has a large amplitude. In conclusion, both the SPaQ and MPS are highly suited to improve understanding SPION behavior, which will lead to the radical improvement of sentinel node biopsy accuracy.

I. INTRODUCTION

Characterization of superparamagnetic iron oxide nanoparticles (SPIONs) provides invaluable information on their use in biomedical applications, such as MRI,[1] hyperthermia,[2] Magnetic Particle Imaging (MPI),[3] and sentinel node detection.[4] The Superparamagnetic Quantifier (SPaQ) was developed to characterize SPIONs in biological environments, such as blood, tissue, and lymph nodes. This makes it suitable to optimize sentinel node detection. Sentinel node biopsies (SNB) are used to determine the lymph node status of a cancer patient.[5] As a result, it can be determined if the tumor has metastasized, and patient prognosis and treatment can be personalized. During SNB, a tracer material is injected in or close to the tumor. The tracer will follow the natural path through the lymphatic system via mechanical transport, that is, no active targeting. Consequently, the tracer will accumulate in the first nodes it encounters, namely, the sentinel

nodes. The sentinel nodes can then be identified using a dedicated probe[6,7] and examined for metastases following surgical removal.

Traditionally, a radioactive tracer is used, but this has many disadvantages, such as limited worldwide availability and a large logistical burden, due to its limited shelf life and few production sites.[8] Superparamagnetic iron oxide nanoparticles (SPIONs) do not have such drawbacks. When SPIONS are used as a tracer, they can be selectively detected *in vivo* using the Differential Magnetometry (DiffMag) protocol.[9] For *in vivo* SNB, a handheld probe is used.[7] Localization of SPIONs *in vivo* can also be useful in different applications, such as intraoperative assessment of tumor boundaries.[10]

SPION detection can be optimized by matching the magnetic properties of the particle with the excitation parameters of the handheld probe. To achieve this, the magnetization curve of the particles is measured, which will show their nonlinear response to external magnetic fields. There are many ways to measure the magnetization curve. *The goal of this paper is to compare our novel SPaQ to Vibrating Sample Magnetometry* (VSM) *and Magnetic Particle Spectroscopy* (MPS).

A commonly used method to measure magnetization curves is Vibrating Sample Magnetometry (VSM).[11] In Fig. 1, measurements on two types of SPION suspensions are shown. How these measurements are performed is described in Sec. III D. In Fig. 1(a), the entire measured curve (from −4 to +4 T) is shown. Figure 1(b) shows the region of interest (−20 to 20 mT) for handheld detectors. These low fields enable measurements by small coils at room temperature, which is a prerequisite for handheld detection. It can be observed that the magnetic moment of SPIONs changes substantially in this field range. This special behavior is the fingerprint of SPIONs. At higher field strengths, the particles saturate and therefore the magnetic moment remains the same. It is a well-known effect that VSM measurements at low fields cause problems of magnetic remanence in the system when superconducting coils are used.[12] To avoid this problem, the SPaQ was created.

Figure 1(c) shows the derivative of the magnetization curve with respect to the magnetic field (dM/dH). In the SPaQ, copper coils are used allowing the Faraday effect to be exploited. An AC excitation field enables direct measurement of the derivative of the magnetization curve (dM/dH), which is related to the point spread function (PSF) in MPI.[13]

In the SPaQ, an excitation field with a low AC amplitude is combined with a gradual DC offset, as can be seen in Fig. 2(a). The magnetization curve, shown in Fig. 2(b), shows the response of the particles to this excitation field. The resultant changing magnetization of the particles is shown in Fig. 2(c). Since our detector measures changes in magnetic flux, the signal obtained by the detector is the derivative of the magnetization; see Fig. 2(d). After the application of a phase-sensitive detection algorithm, dM/dH is found, as shown in Fig. 2(e). Integration yields the magnetization curve, as shown in Fig. 2(f).

A comparable method to the SPaQ is Magnetic Particle Spectroscopy (MPS). This technique was developed to predict the behavior of particles in Magnetic Particle Imaging (MPI)[14] and to optimize their imaging performance. Effort was made to improve sensitivity and signal purity.[15,16] MPS has been used to determine particle parameters, such as core diameter,[14] but also their temperature can be estimated from the produced harmonics.[17] Later, MPS has been used in many biological applications, including measurements on SPIONs in different biological environments,[18] measurements on changes in the magnetization behavior during cellular uptake of SPIONs,[19] and viscosity measurements.[20–22] In many applications, the focus is on the harmonics spectrum. However, in this paper, the focus is on the time signal, which contains both the fundamental frequency and higher harmonics. The time signal represents the magnetization curve. A recent MPS setup at the Technical University of Braunschweig is described. This device can measure dM/dH using Faraday detection, which is similar to SPaQ measurements.

The principle of MPS measurements is shown in Fig. 3, which is similar to Fig. 2. As can be seen in Fig. 3(a), an excitation field of high amplitude is used in MPS. This results in a more dynamic measurement of the magnetization curve compared to the SPaQ measurements, which leads to hysteresis, as can be seen in Fig. 3(f). This phenomenon will be explained in detail later.

Although SPaQ and MPS look at a first glance very similar—in both cases, the nanoparticles are excited by a combination of sinusoidal and static magnetic fields and the magnetic moment of the sample is detected using (gradiometric)

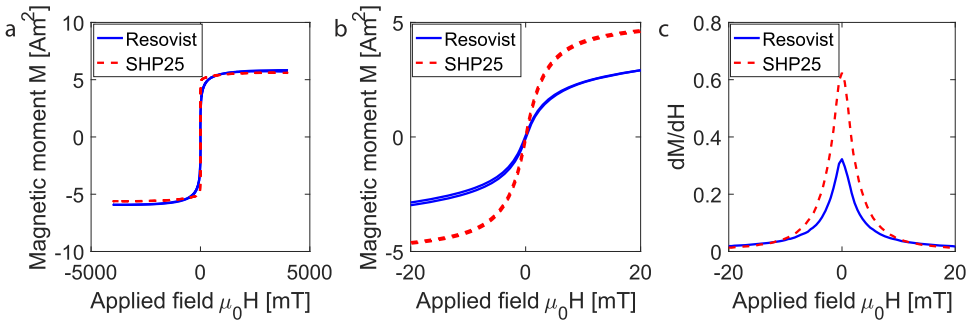

FIG. 1. VSM measurements on two types of SPION suspensions: Resovist and SHP-25. (a) The measured magnetization curve, between −4 and 4 T. (b) A zoomed-in view of curve (a): this is the region of interest for handheld detection, showing the fingerprint of SPIONs. (c) The derivative of curve (b), showing changes in the magnetization of the particle.

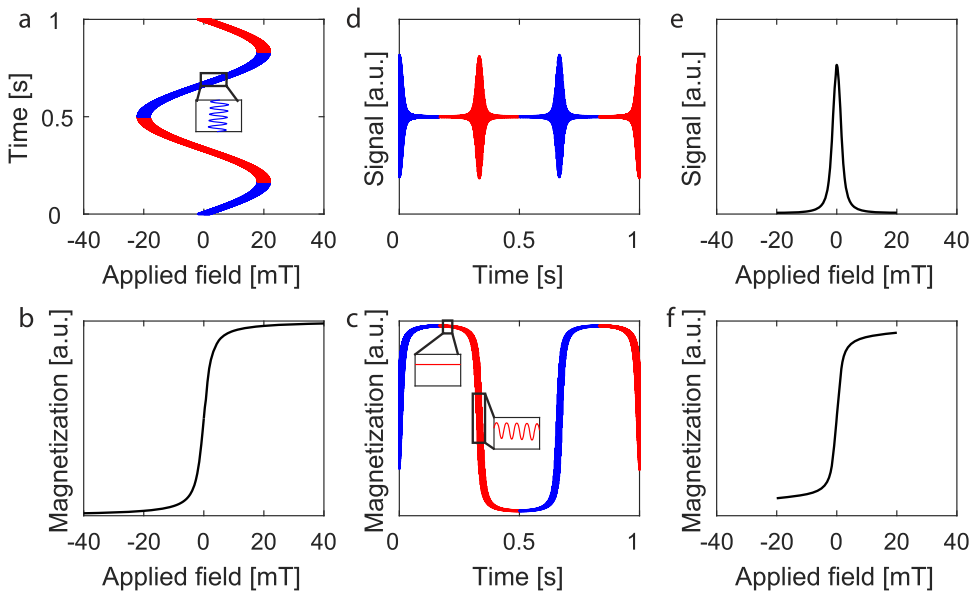

FIG. 2. Schematic overview of SPaQ measurements. (a) A continuous AC magnetic field and changing DC offset are applied to the nanoparticles. (b) The response of the particles is given by their magnetization curve. (c) The resulting magnetization of the particles over time. (d) The resulting signal is the changing magnetization. (e) The envelope of the signal is found by phase-sensitive detection; this is the derivative of the magnetization curve in two directions (which are almost identical). (f) Integration yields the magnetization curve. Blue and red indicate the direction in which the curve is measured.

detection coils—there are a number of differences. In SPaQ, generally a small-amplitude AC field is applied, while the DC field is gradually ramped. In MPS, one generally applies a larger-amplitude AC magnetic field with an optionally superimposed DC magnetic field. While in SPaQ only the fundamental frequency of the detection signal is analyzed, MPS employs the whole harmonic spectrum caused by the nonlinearity of the magnetization curve. The analysis of the whole harmonic spectrum puts much stronger demands on the transmit circuitry, making nanoparticle detection in a clinical setting much more complicated.

Many parameter values can be deduced from the curve measured in either the SPaQ or MPS, such as the core diameter, hydrodynamic diameter, and anisotropy of the particles,[23] but information about the environment of the particles can also be obtained.[20–22] During the design of SPIONs, it is essential to apply a consistent characterization technique. As a result, it will become possible to check quickly what the effect is of a change in the design process. For example, the chemicals used and their precursor concentrations and the temperature and alkalinity of the medium are factors that influence the particles produced and their magnetic properties.[24]

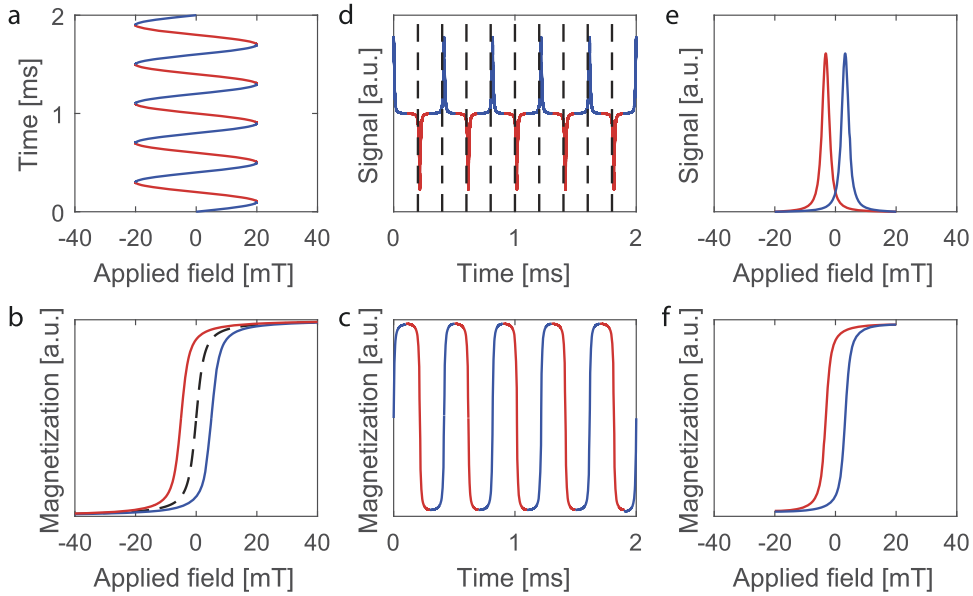

FIG. 3. Schematic overview of MPS measurements. (a) A continuous AC magnetic field is applied to the nanoparticles. (b) The response of the particles is given by their magnetization curve. (c) The resulting magnetization of the particles over time. (d) The resulting signal is the changing magnetization. The black dashed lines show the points where the AC magnetic field passes zero. (e) Averaging gives the derivative of the magnetization curve. (f) Integration leads to the magnetization curve. Blue and red indicate the direction in which the curve is measured.

Another application of particle characterization is the measurement of SPIONs in biological systems. If SPIONs are injected into the blood, a process referred to as protein corona formation will occur.[25] Both the SPaQ and MPS can be used to frequently measure the hydrodynamic diameter of the particles, and as a result, the dynamic process of corona formation can be studied in detail.

An additional biomedical application of SPIONs is in controlled drug delivery. By measuring dM/dH, as long as it contains information on particle dynamics, it becomes possible to check if the drug is bound to the particle.[26]

II. MATERIALS

In this paper, two types of particles were used: Resovist® (Bayer Schering Pharma GmbH) and SHP-25 (Ocean Nanotech). Resovist is a multi-core particle system that has complex structural and magnetic properties, and it is frequently used in MPI.[27,28] SHP-25 is a single-core magnetite nanoparticle that has a core diameter of 25 nm.[29] Both samples were diluted to a concentration of 5 mg(Fe)/ml. For the VSM measurements, small samples of 15 μl were used since larger samples were both too large in size and gave too much signal. For the SPaQ and MPS measurements, samples of 150 μl were used.

III. METHODS

A. SPaQ

1. Device

The SPaQ setup, comprising a co-axial magnetometer, was developed at the University of Twente and consists of several parts. A data acquisition (DAQ) card (NI USB-6289) is used to enable communication with a personal computer (PC). The DAQ card also controls the power amplifier (Servowatt DCP390/60C 50V/8A). The current produced by using the power amplifier is sent through an excitation coil to generate a magnetic field. The unit containing the coils is shown in Fig. 4, and specifications of the coils are given in Table I. The detection coil is designed differentially so as to suppress the induction signal generated by the excitation field (80 dB attenuation). The sample, with a maximum diameter of 23 mm, is placed inside the upper pickup coil. The current measured by the pickup coils is sent through a low-noise differential preamplifier (Krohn-Hite, model 7000, serial LM242), which amplifies the signal by a factor of 10 and applies a low-pass filter that has a cutoff frequency of 30 kHz, to avoid aliasing in the DAQ card. MATLAB is used to both control the system and process data.

2. Measurement protocol

An AC excitation field ($|H_{AC}|$ = 1.33 mT) in combination with a DC offset ($|H_{DC}| \leq$ 13.3 mT) was applied to the sample, as described in Sec. I. This sequence included five repetitive measurements in both directions over 5 s. The excitation frequency was set to 2.5 or 10 kHz in two separate measurements. Details of the measurement protocol can be found in Table II. To avoid temperature fluctuations, there was a waiting time of 20 min between successive measurements. After acquisition, data were processed in MATLAB. A digital phase-sensitive detection algorithm was applied to determine the amplitude of the measured signal. First, the signal was multiplied by a reference signal, namely, a perfect sine at the measurement frequency of 2.5 or 10 kHz, which was in phase with the measured signal in the software. Second, the signal was multiplied by the reference signal that has been shifted 90° to determine the out-of-phase component. After application of a low pass filter (second order Butterworth filter with a cutoff frequency of 20 Hz), two signals X and Y were obtained. X and Y refer to the in-phase and out-of-phase component of the measured signal. The amplitude of the signal was given by $R = \sqrt{(X^2 + Y^2)}$, which is the derivative of the magnetization curve that we are looking for. Numerical integration resulted in the magnetization curve itself.

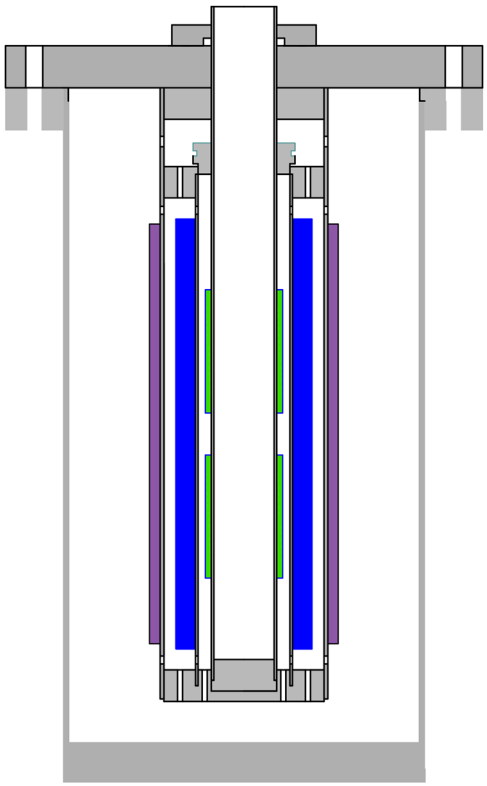

FIG. 4. Schematic representation of the SPaQ. An excitation coil (blue) and a pair of gradiometer detection coils (green) surround a 23 mm diameter sample bore. Samples are placed in the topmost detection coil, which has a homogeneous field region of 2.5 cm along the vertical axis; in this region, the field deviates no more than 5%. The excitation coil generates both the AC and DC excitation fields. An outer field coil (purple) is wound around the main excitation coils. This coil is used for the same purpose as a shielding coil in an MRI system, namely, both to provide shielding to limit the strength of the magnetic field outside the coils and to improve homogeneity of the field inside the coils.

TABLE I. Coil specifications of the SPaQ setup.

	Wire ⌀ (mm)	Inner ⌀ (mm)	Coil length (mm)	Turns [No.]	Resistance (Ω)
Upper pickup coil	0.115	25	47	1800	400
Lower pickup coil	0.115	25	47	1800	400
Inner field coil	1.75	37	164	374	0.72
Outer field coil	1.75	50	160	160	0.48

B. MPS

1. Device

The custom-built MPS setup[30] provides several selectable excitation frequencies between 100 Hz and 25 kHz and magnetic excitation field strengths of up to $\mu_0 H$ = 30 mT of an AC excitation field and an optional superimposed DC offset field. A DAQ card (NI PCI-6733) is used to generate a sinusoidal excitation signal, which is amplified using an AE Techron 7224 power amplifier and sent through the excitation coil. A detection coil is used to measure the change in the magnetization over time. Since the detection coil is designed differentially, the induction signal generated by the excitation field is suppressed (70 dB attenuation) and the fundamental component produced by the particles can be measured. The induced signal in the detection coil is pre-amplified (2×) by using a custom-built pre-amplification module. The amplified induction signal is then acquired via a synchronized DAQ card (NI PCI-6133).

2. Measurement protocol

The excitation field amplitude was set to 25 mT to achieve a sufficient saturation of the particle suspension. The samples were measured at excitation frequencies of 2.5 and 10 kHz in two separate measurements. The total measurement time was set to 0.5 s, leading to 1250 and 5000 periods and therefore 1250 and 5000 averages of the dM/dH curve for the 2.5 and 10 kHz frequencies, respectively. The sampling frequency was set to 2 MS/s which covers 800 samples per period. M(H) curves were reconstructed by integration of the received signal. For that purpose, the acquired induction signal $dU/dt \approx dM/dt$ was summed up cumulatively over time and split into sets of rising and falling edges of the resulting M(t) curve. All rising and falling edges were averaged and plotted over H(t), which was measured indirectly by the coil current and multiplied by the coil constant of the AC excitation coil.

TABLE II. Settings of SPaQ and MPS measurements.

	SPaQ	MPS
AC frequency	2.5 or 10 kHz	2.5 or 10 kHz
AC amplitude	1.33 mT	25 mT
DC frequency	1.1 Hz	-
Maximum DC offset	13.3 mT	-
Measurement time	5 s	0.5 s
Averages	5	1250 or 5000
Sampling frequency	160 kS/s	2 MS/s

C. ACS

AC susceptibility (ACS) measurements were performed using a low-frequency (10 Hz–10 kHz) and a high-frequency (200 Hz–1 MHz) setup at the Technical University of Braunschweig, at AC field amplitudes of 450 and 90 μT, respectively.[31,32] Spectra are the averages of 5 (low-frequency) and 20 (high-frequency) single frequency sweeps and merged to form a single spectrum. Both systems are calibrated and provide data in volume susceptibility.

Spectra were analyzed by applying a generalized Debye model, described by Ludwig *et al.*[32,33] For the distributions of core $f(d_c)$ and hydrodynamic $f(d_h)$ diameters, lognormal distributions are assumed. To limit the number of free fitting parameters (μ_c, σ_c, K, μ_h, and σ_h), 25 nm for SHP-25 and 24.5 nm for Resovist are assumed for the median core diameter; for the standard deviations, σ_c = 0.2 and 0.25 are used as typical values for the particle systems. Note that the core parameters for Resovist are based on the analysis of static M(H) curves.[27,34] In these papers, the authors found that there is a bimodal distribution of magnetic moments: the smaller one corresponds to individual iron oxide cores with diameters between 5 and 8 nm, while the larger one with an effective diameter of around 25 nm is caused by aggregates.

D. VSM

The Quantum Design Physical Property Measurement System (PPMS) installed at the University of Twente was used to perform VSM measurements. The field was swept between −4 and +4 T (starting at 0 T) at various speeds. Between ±4 and ±0.5 T, a continuous sweep at a sweep rate of 20 mT/s was applied. Between ±0.5 T and ±50 mT, the sweep rate was 2 mT/s. Between ±50 mT, a linear step (driven at each field) of 0.5 mT field increment was applied, with each step averaged over 1 s, leading to an accurate measurement in the region of interest. The sample was vibrated at the standard frequency and amplitude settings of 40 Hz and 2 mm. One complete measurement took about 3 h.

Furthermore, since the VSM is not only sensitive to the superparamagnetic sample but also sensitive to the sample holder, its linear contribution has to be removed. This was achieved by correcting for the linear trend that was observed between ±3 and ±4 T, where the particles are assumed to be completely saturated.

It is a well-known problem that the VSM does not perform optimally at low fields around 0 T. Magnetic remanence results in an opening in the magnetization curve,

which looks like hysteresis, but the loop appears in the opposite direction to what is physically expected.[12] To compensate for this, a calibration sample (palladium reference sample, Quantum design, serial no.: PD-1206) was measured by applying the same protocol. The horizontal deviation of the curve at 0 T was determined and used to correct the sample measurements. Finally, the correction was applied by shifting the measurements horizontally to close the loop.

IV. RESULTS

Figure 5 shows the SPaQ measurements. It can be observed that measurements in both directions are almost identical, indicating minor hysteresis. Furthermore, in Fig. 5(a), it can be seen that the amplitude of the peak of the SHP-25 curve is 1.9 times the amplitude of the peak of the Resovist curve.

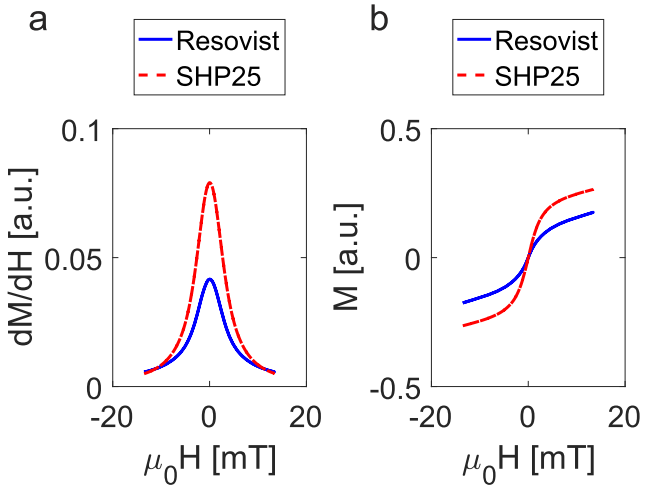

FIG. 5. SPaQ results, measured on Resovist and SHP-25 samples containing 750 μg iron in a total volume of 150 μl at an excitation frequency of 2.5 kHz. (b) is a numerical integration of (a).

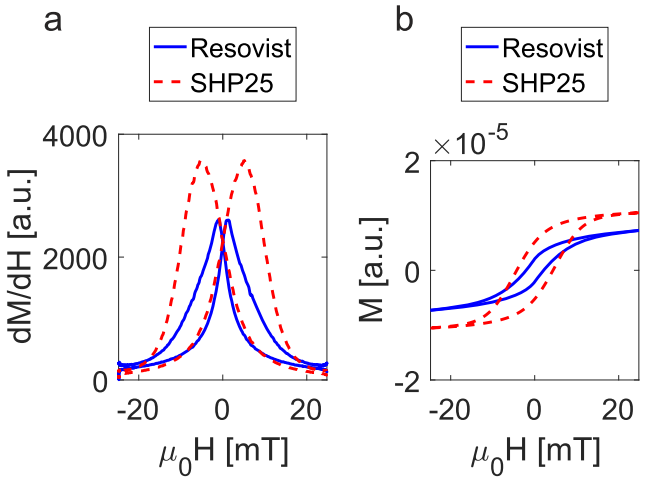

FIG. 6. MPS results, measured on Resovist and SHP-25 samples containing 750 μg iron in a total volume of 150 μl at an excitation frequency of 2.5 kHz. (b) is a numerical integration of (a).

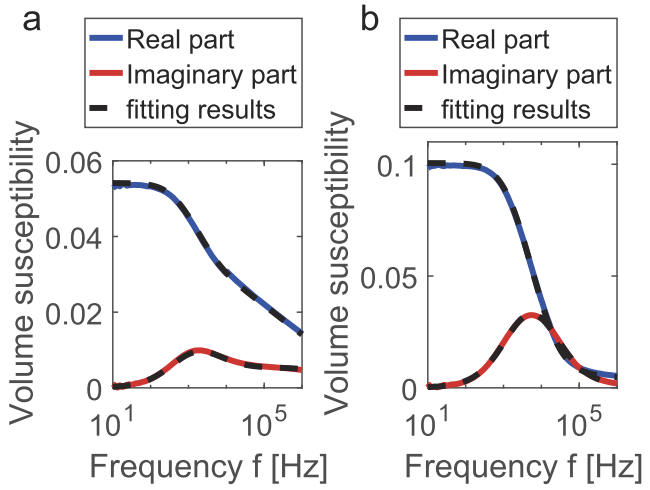

FIG. 7. ACS results, measured on Resovist (a) and SHP-25 (b) samples containing 750 μg iron in a total volume of 150 μl.

The MPS results are shown in Fig. 6. In these measurements, clear hysteresis is visible. The amplitude of the peak of the SHP-25 curve shown in Fig. 6(a) is 1.4 times the amplitude of the peak of the Resovist curve. The width of the hysteresis loop is 10.4 mT for SHP-25 and 2.4 mT for Resovist.

ACS measurements are shown in Fig. 7. Samples of SHP-25 and Resovist show a pronounced Brownian maximum in the imaginary part, indicating that—at least in the low-field

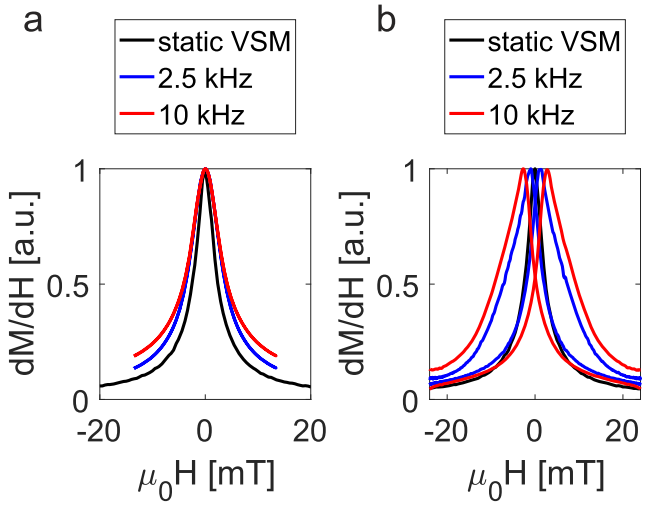

FIG. 8. (a) SPaQ and (b) MPS results, compared with the static VSM curve. Curves were measured at different frequencies (2.5 and 10 kHz), and resulting curves were normalized. Measured on a Resovist sample containing 750 μg iron in a total volume of 150 μl.

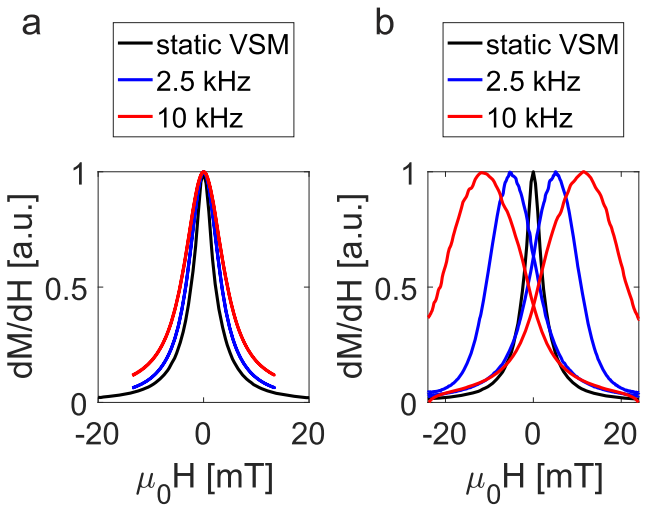

FIG. 9. (a) SPaQ and (b) MPS results, compared with the static VSM curve. Curves were measured at different frequencies (2.5 and 10 kHz), and resulting curves were normalized. Measured on an SHP-25 sample containing 750 μg iron in a total volume of 150 μl.

range—a major proportion of the nanoparticles are thermally blocked. For SHP-25, the maximum is at 5.7 kHz, whereas for Resovist it is at 1.8 kHz. For Resovist, the imaginary part shows a shallow shoulder at frequencies above the Brownian peak, while the real part shows a rather shallow decay compared to SHP-25. This is a clear indication of a large contribution from Néel-dominated nanoparticles. The high-frequency shoulder for Resovist also causes a higher harmonics spectrum at higher frequencies in MPS.

MPS and SPaQ measurements at different AC frequencies are shown in Figs. 8 and 9 for Resovist and SHP-25 particles, respectively. All curves are normalized and compared to the VSM measurements.

V. DISCUSSION

Both the SpaQ and MPS provide accurate measurements of the magnetization curve, and both are superior to VSM in this field range (between ±25 mT). The measurements are much faster, do not require correction, and can be conducted at room temperature.

Both the SPaQ and MPS give broadly similar information and can therefore be used in similar applications. These devices provide crucial information on many applications, such as controlled drug delivery and studying the dynamic protein corona formation process, but also on the design process of SPIONs. However, in sentinel node biopsies, it is preferable to use the SPaQ due to its intrinsic similarities with DiffMag. Also, the described SPaQ setup has a large sample holder, which allows measurements on entire lymph nodes. The direct correlation between MPS and MPI makes MPS the best choice for predicting particle behavior in MPI.

As mentioned in the Introduction, the main difference between SPaQ and MPS measurements lies in the excitation sequence and the detection scheme used. The SPaQ measurements look remarkably similar to static VSM measurements. However, in VSM measurements, the sample vibrates in a homogeneous field. Even though the AC amplitude in the SPaQ is low, the particles do experience a changing magnetic field. Therefore, particle dynamics will slightly influence such measurements. If particles experience a sufficiently short relaxation time, nearly no hysteresis is observed in the measured curves. However, due to their large AC amplitudes, MPS measurements are more dynamic and consequently more sensitive to particle dynamics compared to SPaQ measurements, as indicated by the hysteresis revealed in the measured curves. In addition, SPaQ analyzes the magnitude of the fundamental frequency only, while MPS also explores phase information.

The strength of the SPaQ over MPS is its freedom to adjust measurement parameters. In the SPaQ, a small AC field is combined with a gradual DC offset. Therefore, the AC amplitude can be varied, without influencing the total range (maximum field) in which the magnetization curve is measured. On the contrary, in MPS, the large AC amplitude determines the range in which the magnetization curve is measured. Measuring at various AC amplitudes is valuable when SPaQ measurements are used to predict the DiffMag response of the particle. The various amplitudes will represent various distances to the handheld probe that is used in DiffMag. For DiffMag, only small field strengths are needed since the particles respond to fields as low as 1 mT. This makes DiffMag suitable for safe use in patients. Little energy is needed, and it becomes possible to generate a handheld system with limited heating of the probe.

Another advantage of the SPaQ over MPS is its freedom to select an arbitrary excitation frequency. In MPS, a resonant circuit is needed to generate sufficiently high magnetic field strengths. Therefore, it is only possible to measure at certain discrete frequencies. However, due to the small AC amplitude in the SPaQ, it is possible to select various frequencies without changes in hardware. Consequently, it is much easier to sweep the frequency in the SPaQ compared to MPS.

The nature of the sample (which and how many particles are used) influences the height (magnetic susceptibility) and width (or slope, field strength at which the particles saturate) of the measured curve. In MPS, the distance between the peaks (that is the width of the hysteresis loop) changes as well, which is dependent on the relaxation time of the particles.[35–37]

In the ACS measurements, it was shown that both particles show an optimal response at a frequency below 10 kHz. Both Brownian and Néel relaxation times depend on the AC and DC magnetic field amplitudes and decrease with increasing field.[29] Consequently, the susceptibility spectra will be shifted to higher frequencies in SPaQ or MPS measurements. Additionally, an increase in field amplitude causes the generation of higher harmonics, which leads to a bending of the magnetization curve. Along with particle dynamics, this results in the hysteresis loop that was observed in the MPS measurements.

The influence of particle dynamics is shown by measuring at various frequencies, as shown in Figs. 8 and 9. The frequency effect is largest in MPS measurements, but it can be seen that there is a slight influence of particle dynamics in SPaQ measurements as well. As can be seen, the frequency effect is larger for SHP-25 compared to Resovist, which accords with the steep decay with increasing frequency observed in the ACS measurements.

VI. CONCLUSION

In conclusion, both the SPaQ and MPS are capable of measuring a magnetization curve at low field strengths (<25 mT). Both methods are superior to VSM measurements because they are much faster, can be conducted at room temperature, and do not need a correction. Measuring the magnetization curve reliably can give invaluable information about SPIONs and their dynamics, which will improve many applications, including sentinel node biopsies. There are also differences between the SPaQ and MPS. Due to the much larger AC field amplitude, MPS is very sensitive to particle dynamics. The lower AC field amplitude in the SPaQ strongly simplifies the electronics, reduces heating, and allows a continuous choice of frequency.

VII. FUTURE WORK

To optimize SPaQ and MPS measurements, two main improvements need to be made. First, it is vital to calibrate both systems. As a result, the magnetic moment of the sample can be calculated from the measured voltage.

Second, the thermal stability of the SPaQ needs to be improved, which we intend to work on. Heating of the excitation coil leads to temperature fluctuations throughout the system, reducing the reproducibility of measurements. Thermal stability can be improved by making key changes to the design.

In addition, it is essential to measure particles in various environments (for example, in media of various viscosities) in the SPaQ. This will give more insight into the effect of particle dynamics on the measurements. For a sentinel node biopsy, it is essential to know how the magnetic behavior of the particles changes while trapped inside a lymph node. When particles accumulate in a lymph node, they will be partially immobilized due to macrophage uptake. This will increase the relaxation time and therefore reduces the measured detector voltage. Consequently, it might seem that there are fewer particles in the lymph node and the node might be classified incorrectly (for example, classified as a normal node instead of a sentinel node).

ACKNOWLEDGMENTS

Financial support from the Netherlands Organization for Scientific Research (NWO), under the research program Magnetic Sensing for Laparoscopy (MagLap) with Project No. 14322, and from the German Research Foundation DFG via SPP1681 under Grant Nos. SCHI-383/2-1 and VI-892/1-1 are gratefully acknowledged.

REFERENCES

[1]D. Stanicki, L. V. Elst, R. N. Muller, S. Laurent, D. Felder-Flesch, D. Mertz, A. Parat, S. Begin-Colin, G. Cotin, J.-M. Greneche, O. Ersen, B. Pichon, V. Socoliuc, V. Kuncser, R. Turcu, L. Vekas, P. Fosterh, and R. Bartha, in *Contrast Agents for MRI: Experimental Methods*, edited by V. C. Pierre and M. J. Allen (The Royal Society of Chemistry, 2018), Chap. 4, pp. 318–447.
[2]T. L. Kalber, K. L. Ordidge, P. Southern, M. R. Loebinger, P. G. Kyrtatos, Q. A. Pankhurst, M. F. Lythgoe, and S. M. Janes, Int. J. Nanomed. **11**, 1973 (2016).
[3]N. Panagiotopoulos, R. L. Duschka, M. Ahlborg, G. Bringout, C. Debbeler, M. Graeser, C. Kaethner, K. Lüdtke-Buzug, H. Medimagh, J. Stelzner, T. M. Buzug, J. Barkhausen, F. M. Vogt, and J. Haegele, Int. J. Nanomed. **10**, 3097 (2015).
[4]A. Karakatsanis, K. Daskalakis, P. Stålberg, H. Olofsson, Y. Andersson, S. Eriksson, L. Bergkvist, and F. Wärnberg, Br. J. Surg. **104**, 1675 (2017).
[5]A. Giuliano and A. Gangi, Breast J. **21**, 27 (2015).
[6]M. Kaneko, K. Ohashi, S. Chikaki, A. Kuwahata, M. Shiozawa, M. Kusakabe, and M. Sekino, AIP Adv. **7**, 056713 (2017).
[7]S. Waanders, M. Visscher, R. R. Wildeboer, T. O. B. Oderkerk, H. J. G. Krooshoop, and B. Ten Haken, Phys. Med. Biol. **61**, 8120 (2016).
[8]M. Ahmed, A. D. Purushotham, and M. Douek, Lancet Oncol. **15**, e351 (2017).
[9]M. Visscher, S. Waanders, H. Krooshoop, and B. ten Haken, J. Magn. Magn. Mater. **365**, 31 (2014).
[10]R. X. Xu, J. S. Xu, J. Huang, M. F. Tweedle, C. Schmidt, S. P. Povoski, and E. W. Martin, Proc. SPIE **7556**, 75560T (2010).
[11]M. S. Lubell and A. S. Venturino, Rev. Sci. Instrum. **31**, 207 (1960).
[12]Quantum_Design, "Application note 1070-207. Using PPMS superconducting magnets at low fields," Application Note 1070-207, 2009.
[13]I. Schmale, J. Rahmer, B. Gleich, J. Borgert, and J. Weizenecker, in *Magnetic Particle Imaging: A Novel SPIO Nanoparticle Imaging Technique*, edited by T. M. Buzug and J. Borgert (Springer Berlin Heidelberg, Berlin, Heidelberg, 2012), pp. 287–292.
[14]S. Biederer, T. Knopp, T. Sattel, K. Lüdtke-Buzug, B. Gleich, J. Weizenecker, J. Borgert, and T. Buzug, J. Phys. D: Appl. Phys. **42**, 205007 (2009).
[15]M. Graeser, T. Knopp, M. Grüttner, T. F. Sattel, and T. M. Buzug, Med. Phys. **40**, 42303 (2013).
[16]D. B. Reeves and J. B. Weaver, J. Phys. D: Appl. Phys. **47**, 45002 (2014).
[17]A. M. Rauwerdink, E. W. Hansen, and J. B. Weaver, Phys. Med. Biol. **54**, L51 (2009).
[18]N. Löwa, M. Seidel, P. Radon, and F. Wiekhorst, J. Magn. Magn. Mater. **427**, 133 (2017).
[19]W. Poller, N. Löwa, F. Wiekhorst, M. Taupitz, S. Wagner, K. Möller, G. Baumann, V. Stangl, L. Trahms, and A. Ludwig, J. Biomed. Nanotechnol. **12**, 337 (2016).
[20]A. M. Rauwerdink and J. B. Weaver, J. Magn. Magn. Mater. **322**, 609 (2010).
[21]T. Yoshida, S. Bai, A. Hirokawa, K. Tanabe, and K. Enpuku, J. Magn. Magn. Mater. **380**, 105 (2015).
[22]S. Draack, N. Lucht, H. Remmer, M. Martens, B. Fischer, M. Schilling, F. Ludwig, and T. Viereck, "Multiparametric magnetic particle spectroscopy of $CoFe_2O_4$ nanoparticles in viscous media" (unpublished).
[23]D. Reeves and J. Weaver, Appl. Phys. Lett. **107**, 223106 (2015).
[24]R. Hufschmid, H. Arami, R. Ferguson, M. Gonzales, E. Teeman, L. Brush, N. Browning, and K. Krishnan, Nanoscale **7**, 11142 (2015).
[25]P. Pino, B. Pelaz, Q. Zhang, P. Maffre, G. Nienhaus, and W. Parak, Mater. Horiz. **1**, 301 (2014).
[26]N. Hamzian, M. Hashemi, M. Ghorbani, M. H. Bahreyni Toosi, and M. Ramezani, Iran. J. Pharm. Res. **16**, 8 (2017).
[27]D. Eberbeck, F. Wiekhorst, S. Wagner, and L. Trahms, Appl. Phys. Lett. **98**, 182502 (2011).
[28]T. Yoshida, K. Enpuku, F. Ludwig, J. Dieckhoff, T. Wawrzik, A. Lak, and M. Schilling, in *Magnetic Particle Imaging: A Novel SPIO Nanoparticle Imaging Technique*, edited by T. M. Buzug and J. Borgert (Springer Berlin Heidelberg, Berlin, Heidelberg, 2012), pp. 3–7.

[29]J. Dieckhoff, D. Eberbeck, M. Schilling, and F. Ludwig, J. Appl. Phys. **119**, 043903 (2016).
[30]S. Draack, T. Viereck, C. Kuhlmann, M. Schilling, and F. Ludwig, Int. J. Magn. Particle Imaging **3**(1), 1703018 (2017).
[31]F. Ludwig, A. Guillaume, M. Schilling, N. Frickel, and A. M. Schmidt, J. Appl. Phys. **108**, 33918 (2010).
[32]F. Ludwig, C. Balceris, T. Viereck, O. Posth, U. Steinhoff, H. Gavilan, R. Costo, L. Zeng, E. Olsson, C. Jonasson, and C. Johansson, J. Magn. Magn. Mater. **427**, 19 (2017).
[33]F. Ludwig, C. Balceris, C. Jonasson, and C. Johansson, IEEE Trans. Magn. **53**, 6100904 (2017).
[34]T. Yoshida, N. B. Othman, and K. Enpuku, J. Appl. Phys. **114**, 173908 (2013).
[35]L. R. Croft, P. W. Goodwill, and S. M. Conolly, IEEE Trans. Med. Imaging **31**, 2335 (2012).
[36]M. Utkur, Y. Muslu, and E. U. Saritas, Phys. Med. Biol. **62**, 3422 (2017).
[37]C. Kuhlmann, A. P. Khandhar, R. M. Ferguson, S. Kemp, T. Wawrzik, M. Schilling, K. M. Krishnan, and F. Ludwig, IEEE Trans. Magn. **51**, 1 (2015).